

A CONCEPTUAL DESIGN OF CIRCULAR HIGGS FACTORY*

Yunhai Cai[†], SLAC National Accelerator Laboratory, Menlo Park, CA 74024, USA

Abstract

Similar to a super B-factory, a circular Higgs factory will require strong focusing systems near the interaction points and a low-emittance lattice in the arcs to achieve a factory luminosity. At electron beam energy of 125 GeV, beamstrahlung effects during the collision pose an additional challenge to the collider design. In particular, a large momentum acceptance at the 2 percent level is necessary to retain an adequate beam lifetime. This turns out to be the most challenging aspect in the design of a circular Higgs factory. In this paper, an example will be provided to illustrate the beam dynamics in a circular Higgs factory, emphasizing the chromatic optics. Basic optical modules and advanced analysis will be presented. Most importantly, we will show that 2% momentum aperture is achievable.

INTRODUCTION

Since the discovery of the Higgs particle at LHC, the recent results for ATLAS and CMS have shown that the discovered particle resembles the Higgs boson in the standard model of elementary particles. Because of this remarkable discovery, it becomes increasingly important to precisely measure the property of the particle that gives the mass to all and to study the nature of the spontaneous symmetry breaking in the standard model.

The relatively low mass of the Higgs boson provides an opportunity to build an e^+ and e^- collider to efficiently and precisely measure its properties. In the production channel of $e^+e^- \rightarrow HZ$, the beam energy required for such a collider is 125 GeV, which is about 20% higher than the energy reached about two decades ago at LEP2. Can we design and build a circular Higgs factory (CHF) within a decade? What are the major challenges in the design? In this paper, we will address these questions.

LUMINOSITY

In a collider, aside from its energy, its luminosity is the most important design parameter. For Gaussian beams, we can write the bunch luminosity as

$$\mathcal{L}_b = f_0 \frac{N_b^2}{4\pi\sigma_x\sigma_y} R_h, \quad (1)$$

where f_0 is the revolution frequency, N_b the bunch population, $\sigma_{x,y}$ transverse beam sizes, and R_h is a factor of geometrical reduction due to a finite bunch length σ_z and is given by

$$R_h = \sqrt{\frac{2}{\pi}} a e^{a^2} K_0(a^2), \quad (2)$$

$a = \beta_y^*/(\sqrt{2}\sigma_z)$, β_y^* is the vertical beta function at the interaction point (IP), and K_0 the modified Bessel function. In order to prevent R_h from becoming too small, we shall require $\sigma_z \approx \beta_y^*$. Obviously, for a number of n_b bunches, the total luminosity is $\mathcal{L} = n_b \mathcal{L}_b$.

In general, the beam sizes in the luminosity formula are not static variables. They are subject to the influence of the electromagnetic interaction during the collision. Typically, for flat beams, the vertical beam size will be blown up by the beam-beam force. To take this effect into account, we introduce the beam-beam parameter as [1]

$$\xi_y = \frac{r_e N_b \beta_y^*}{2\pi\gamma\sigma_y(\sigma_x + \sigma_y)}, \quad (3)$$

where γ is the Lorentz factor and r_e the classical electron radius. Using this formula for ξ_y , we can rewrite the luminosity as [2]

$$\mathcal{L} = \frac{cI\gamma\xi_y}{2r_e^2 I_A \beta_y^*} R_h, \quad (4)$$

where I is the beam current and $I_A = ec/r_e \approx 17045$ A, the Alfven current. Since ξ_y is limited below 0.1 in most colliders, this formula is often used for estimating an upper bound of the luminosity.

Table 1: Main parameters of a Circular Higgs Factory.

Parameter	LEP2	CHF
Beam energy, E_0 [GeV]	104.5	125.0
Circumference, C [km]	26.7	52.7
Beam current, I [mA]	4	13
SR power, P_{SR} [MW]	11	50
Beta function at IP, β_y^* [mm]	50	1
Hourglass factor, R_h	0.98	0.73
Beam-beam parameter, ξ_y	0.07	0.10
Luminosity/IR, \mathcal{L} [$10^{34} \text{cm}^{-2} \text{s}^{-1}$]	0.0125	2.55

In Table 1, we tabulated a set of consistent parameters for a CHF. In contrast to the B-factories [3,4], the beam current is severely limited by the power of synchrotron radiation at very high energy. To reach the factory luminosity, we need to have very strong final focusing systems and a very low emittance lattice. This combination makes the design of optics much more difficult compared with that of the B-factories.

SYNCHROTRON RADIATION

When an electron is in circular motion with a bending radius ρ , its energy loss per turn to synchrotron radiation is given by

$$U_0 = \frac{4\pi r_e m c^2 \gamma^4}{3\rho}. \quad (5)$$

* Work supported by the Department of Energy under Contract Number: DE-AC02-76SF00515.

[†] yunhai@slac.stanford.edu

This loss has to be compensated by an RF system. The required RF power per ring is

$$P_{SR} = U_0 I / e. \quad (6)$$

For the beam energy of 125 GeV with a bending radius of $\rho = 6.1$ km in arcs, we have $U_0 = 3.56$ GeV. Adding additional bends in the interaction region, it increases to $U_0 = 3.85$ GeV, which means that electron loses about 3.1% of its energy every turn. The loss has to be compensated by the RF cavities. Here we have used a RF system with $f_{RF} = 650$ MHz and $V_{RF} = 8.45$ GV. The voltage also provides the longitudinal focusing to the beam so that its length is not too long comparing to the vertical beta function at the interaction point. Assuming P_{SR} has to be less than 50 MW, the beam current is limited to 13.0 mA in the ring. Applying the expression of P_{SR} to the luminosity formula, we obtain

$$\mathcal{L} = \frac{3c\xi_y\rho P_{SR}}{8\pi r_e^3\gamma^3\beta_y^*P_A}R_h, \quad (7)$$

where $P_A = mc^2I_A/e \approx 8.7$ GW. This scaling property of luminosity in e^+e^- colliders at extremely high energy was given by Richter [5].

For a CHF with beam energy larger than 125 GeV, its beam current will be severely capped by the electrical power consumed by the RF system and therefore a smaller β_y^* seems the only available option to reach the required factory luminosity.

BEAMSTRAHLUNG

Another important aspect of very high energy colliding beams is the emission of photons during collision. In general, this phenomenon is well known and called beamstrahlung. Recently, Telnov found [6] that the most limiting effects to a CHF is an event when a high-energy photon is emitted by an electron in the beamstrahlung process. The electron energy loss can be so large that it falls outside of the momentum aperture η in the colliding ring. For a typical CHF, it was suggested that the following,

$$\frac{N_b}{\sigma_x\sigma_z} < \frac{0.1\eta\alpha}{3\gamma r_e^2}, \quad (8)$$

has to be satisfied to achieve 30 minutes of beam lifetime. Here $\alpha \approx 1/137$ is the fine structure constant. If we introduce aspect ratios of beta functions at the IP and emittances in the ring, namely $\kappa_\beta = \beta_y^*/\beta_x^*$ and $\kappa_e = \epsilon_y/\epsilon_x$, this criteria can be rewritten as

$$\frac{N_b}{\sqrt{\epsilon_x}} < \frac{0.1\eta\alpha\sigma_z}{3\gamma r_e^2} \sqrt{\frac{\beta_y^*}{\kappa_\beta}} \quad (9)$$

On the other hand, to achieve the beam-beam parameter ξ_y , we need

$$\frac{N_b}{\epsilon_x} = \frac{2\pi\gamma\xi_y}{r_e} \sqrt{\frac{\kappa_e}{\kappa_\beta}}. \quad (10)$$

Combining this equation with Eq. (9), we have

$$\epsilon_x < \frac{\beta_y^*}{\kappa_e} \left(\frac{0.1\eta\alpha\sigma_z}{6\pi\gamma^2\xi_y r_e} \right)^2. \quad (11)$$

Since the quantities like ξ_y , β_y^* , and σ_z are largely determined by the required luminosity and γ by the particle to be studied, this inequality specifies a low-emittance lattice that is required to achieve 30 minutes of beam lifetime. Normally, the natural emittance scales as γ^2 . Here it requires a scaling of γ^{-4} , indicating another difficulty in designing a factory with much higher energy beyond 125 GeV.

Table 2: Additional parameters selected to mitigate the beamstrahlung effects so that beamstrahlung beam lifetime is longer than 30 minutes.

Parameter	LEP2	CHF
Beam energy, E_0 [GeV]	104.5	125.0
Circumference, C [km]	26.7	52.65
Horizontal emittance, ϵ_x [nm]	48	4.5
Vertical emittance, ϵ_y [nm]	0.25	0.0045
Momentum acceptance, η [%]	1.0	2.0
Bunch length, σ_z [mm]	16.1	1.85
Momentum compaction, α_p [10^{-5}]	18.5	2.5

As shown in Table 2, we need to design a lattice with much smaller emittance than the one in LEP2 to mitigate the beamstrahlung effect. In particular, to satisfy the condition in Eq.(11), the emittance has to be smaller than 7 nm. Typically, a low emittance lattice requires smaller dispersion and stronger focusing. Both will lead to an increase in the strength of the sextupole, therefore dramatically reducing the dynamic aperture of the storage ring.

In the choice of the main design parameters, we want a factor of 100 increase in luminosity from LEP2. Due to the limit of the electric power, the increase of luminosity is largely achieved by a combination of very small beta functions at the IP and a low emittance lattice. In summary, the lattice of a CHF has the following main challenges:

- Low emittance lattice at high energy
- High packing factor of magnets
- Strong final focusing
- Large momentum acceptance
- Short bunches

A high packing factor is required to reduce synchrotron radiation in the bending magnets and not increase the circumference of the ring. In this design, the dipoles in the arcs occupy 73% of the space in the ring. We will proceed to this specific design to show how to meet these challenges.

ARC

For a simple electron ring, the horizontal emittance is given by

$$\epsilon_x = C_q\gamma^2\theta^3 F_c, \quad (12)$$

where C_q is a constant,

$$C_q = \frac{55}{32\sqrt{3}} \frac{\hbar}{mc}, \quad (13)$$

and $\theta = 2\pi/N_c$ is the bending angle per cell, and N_c the number of cell. F_c depends only on the structure of the cell. For FODO cells with equal phase advances, $\mu_x = \mu_y = \mu$, we have,

$$F_c^{FODO} = \frac{1 - \frac{3}{4} \sin^2 \frac{\mu}{2} + \frac{1}{60} \sin^4 \frac{\mu}{2}}{4 \sin^2 \frac{\mu}{2} \sin \mu}, \quad (14)$$

which is plotted as a function of μ in Fig. 1. For a 60° cell, we have $F_c^{FODO}(\pi/3) = 781/480\sqrt{3} \approx 0.94$.

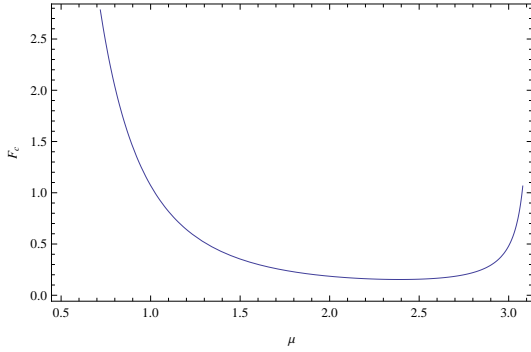


Figure 1: The emittance scaling parameter F_c as a function of phase advance μ in FODO cells.

Clearly, as seen in Eq. (12), the most effective way to reduce the emittance is to make the bending angle in a cell small. That implies that we use more cells. To reach 4 nm emittance, we used $N_c = 1176$.

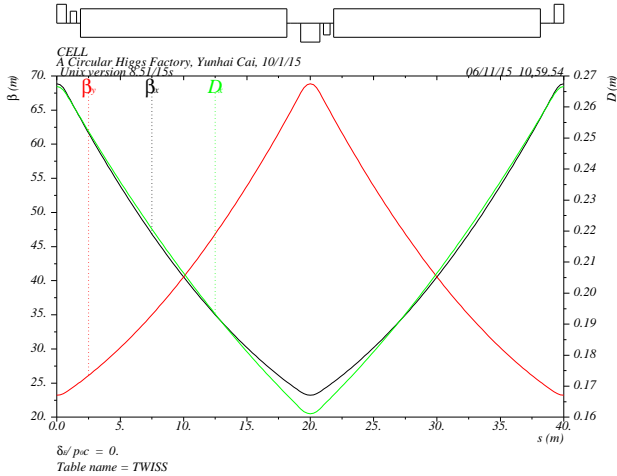


Figure 2: Lattice functions in a 60° FODO cell.

In the arcs, we choose FODO cells because of their high packing factor and use many cells to reach the required emittance. The 60° phase advance is selected due to its property of resonance cancellation that we will explain later. The optics of the cell is illustrated in Fig. 2. Every six cells makes

a unit transformation of betatron oscillation. In our design, each arc consists of 24 units and ends with dispersion suppressors. Similar to LEP2, we have eight arcs and eight straight sections to complete a ring with parameters shown in Table 2.

Table 3: The nonlinear chromaticities and tune shifts due to betatron amplitudes in the lattice that consists of arcs and simple straight sections.

Derivatives of tunes	Values
$\partial v_{x,y}/\partial \delta$	0, 0
$\partial^2 v_{x,y}/\partial \delta^2$	-52, +102
$\partial^3 v_{x,y}/\partial \delta^3$	+1152, +197
$\partial v_x/\partial J_x [m^{-1}]$	-8.43×10^4
$\partial v_{x,y}/\partial J_{y,x} [m^{-1}]$	-3.11×10^5
$\partial v_y/\partial J_y [m^{-1}]$	-5.34×10^4

In this study, we set two families of sextupoles to make the linear chromaticity zero in the ring. For the third-order resonances, the contribution of sextupoles to all driving terms along the storage ring are computed [7] using the Lie method and plotted in Fig. 3. As one can see from the figure, they are all canceled out within one betatron unit (made with six cells), as predicted by theorem [8].

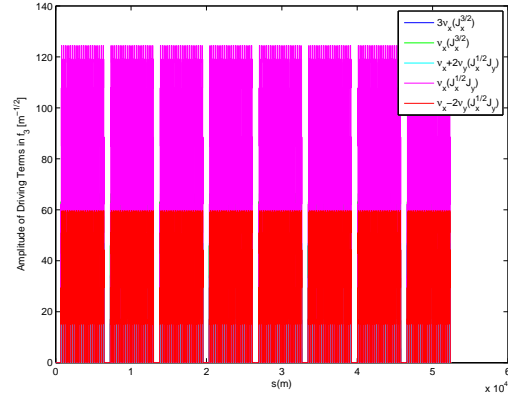


Figure 3: All third-order resonances driven by sextupoles.

For the fourth-order resonances, we find similar cancellations [7] as shown in Fig. 4 except for one resonance: $2v_x - 2v_y = 0$. Since this resonance overlaps the same line as the linear coupling resonance in the betatron tune space, we can ignore it because the ring cannot operate near the linear resonance anyway.

It is also worth noting that there are three more terms of geometric aberrations in f_4 . To quantify their effects on the beam, we compute the tune shifts along with the high-order chromaticities using the normal form analysis [9] and tabulate the result in Table 3. Compared with the existing storage rings, these tune shifts are too large at least by an order of magnitude.

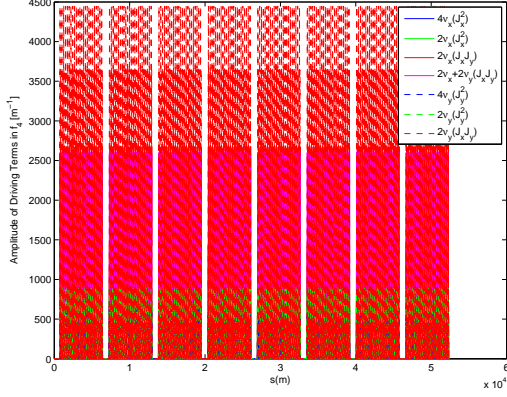


Figure 4: Fourth-order resonances driven by sextupoles.

FINAL FOCUSING SYSTEM

Note that the beam lifetime condition in Eq. (11) does not depend on κ_β . Therefore, according to Eq. (10), κ_β (or β_x^*) can be used to adjust the bunch population N_b or equivalently the number of bunches n_b when the total current is limited by the electrical power. Here we would like to choose a large β_x^* , leading to a smaller n_b . Our choice of the parameters in the interaction region are tabulated in Table 4.

Table 4: Other parameters determined by a specific design of final focusing system.

Parameter	LEP2	CHF
Beam energy, E_0 [GeV]	104.5	125.0
Circumference, C [km]	26.7	52.65
β_x^* [mm]	1500	100
β_y^* [mm]	50	1
Bunch population, N_b [10^{10}]	57.5	7.77
Number of bunches, n_b	4	184

It is always challenging to design a final focusing system (FFS) in a circular collider. In the CHF, it becomes even more so because of a smaller β_y^* (1 mm) and a longer distance L^* (2 meter) which is the distance between the IP and the first focusing quadrupole.

Here we adopt an optics similar to the design of a linear collider. The optics of the FFS is shown in Fig. 5. The FFS starts with a final transformer (FT), continues with a chromatic correction in the vertical (CCY) and then the horizontal plane (CCX), and ends with a matching section. The FFS has two secondary imaging points and fits in a 321-meter section.

The FT contains four quadrupoles, including the final focusing doublet. The betatron phase advances are 180° in both planes. At the end of the FT, we have the first imaging point where the beta functions remain very small.

The CCY consists of four 90° FODO cells and makes a unit of betatron transformer. The module starts at the mid-

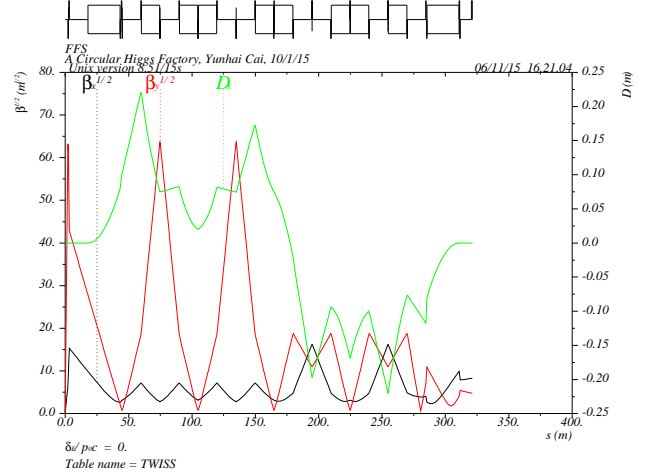


Figure 5: Lattice functions in a final focusing system with local chromatic compensation section.

dle of the defocusing quadrupole to enhance the peak of the vertical beta function at the positions of a pair of sextupoles separated by “-I” transformation. Five dipoles with an equal bending angle provide dispersions at the locations of the sextupoles. At the end of the CCY, we have the second imaging point at which the lattice functions are identical to those at the first one.

Similarly, we construct the CCX, but starting at the middle of the focusing quadrupole. There are five dipoles that generate the dispersion with negative bending angles. The amplitude of the angles are chosen to be the same as those in the CCY so that there is no net bending from the FFS. At the end of the CCX, we have a section matching to the optics of the dispersion suppressor.

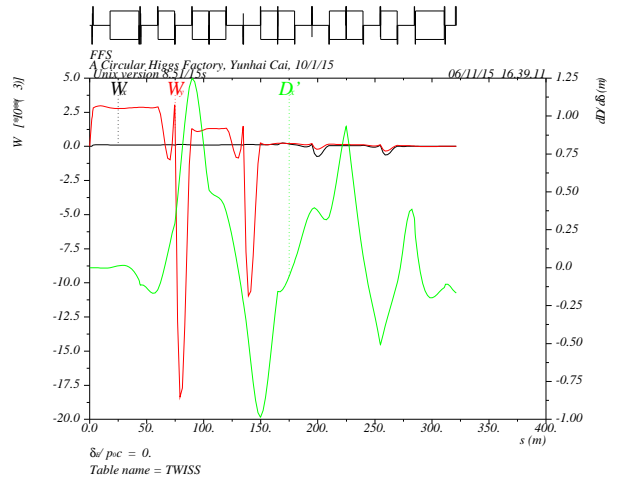


Figure 6: W function and the second order dispersion in the final focusing system with the local chromatic compensation.

The nonlinear chromatic effects can be characterized by the high order derivatives of the lattice functions. These

derivatives can be computed [10] using the technique of the differential algebra [11]. For the FFS, we start with the initial condition: $\beta_x = 0.1$ m and $\beta_y = 1$ mm and calculate the lattice functions and their derivatives element-by-element down to the end.

The first order chromaticity is compensated by two pairs of sextupoles in the CCY and CCX respectively in the horizontal and vertical planes; the second order ones by slight changes of betatron phases between the final doublet and the sextupole pairs; and finally the third order ones by the two sextupoles at the two secondary imaging points where the beta functions are at the minimum. The results of the chromatic compensation is summarised in Table 5. Clearly, the nonlinear chromatic effects in the FFS have been reduced to similar values as in the arcs shown in Table 3. In addition, we plot the W functions and the second order dispersion in Fig. 6. It is worth noting that there is a small amount of second order dispersion leaking out of the FFS.

Table 5: The chromatic tune shifts from the FFS after the correction.

Derivatives of tunes	Values
$\partial\nu_{x,y}/\partial\delta$	-0.43, -0.34
$\partial^2\nu_{x,y}/\partial\delta^2$	+127, +49
$\partial^3\nu_{x,y}/\partial\delta^3$	-954, -852

COLLIDER

Replacing two interaction regions with two simple straights in the arc lattice, we build a collider lattice shown in Fig. 7. The main parameters are summarized in Table 6. Since the lattice has a two-fold symmetry, the half of the betatron tunes are slightly above the half integer, which enhances the dynamic focusing from the beam-beam interaction. As a result, the beam-beam parameter becomes larger as demonstrated in the B-factories [3, 4].

Table 6: Main parameters of the Circular Higgs Factory.

Parameter	Value
Energy, E_0 [GeV]	125.0
Circumference, C [km]	52.7
Tune, ν_x, ν_y, ν_z	225.04, 227.14, 0.165
Natural emittance, ϵ_x [nm]	4.5
Bunch length, σ_z [mm]	1.85
Energy spread, σ_δ	1.44×10^{-3}
Momentum compaction	1.25×10^{-5}
Damping time, τ_x, τ_y, τ_z [ms]	11.4, 11.4, 5.7
Energy loss per turn, U_0 [GeV]	3.85
RF voltage, V_{RF} [GV]	8.45
RF frequency, f_{RF} [MHz]	650.0
Harmonic number	114144

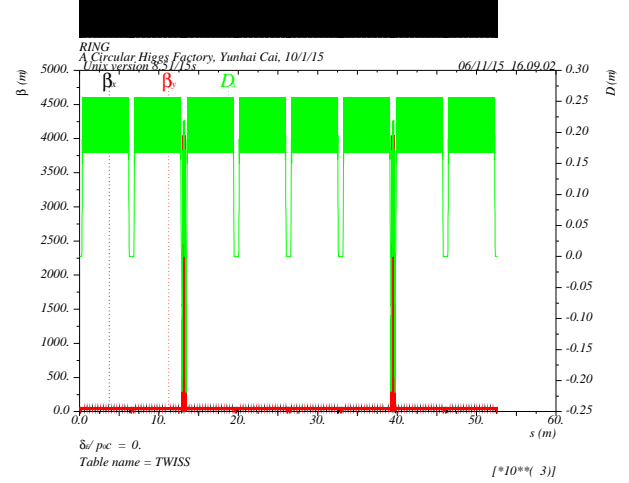


Figure 7: Lattice functions in the CHF that includes two interaction regions.

Since the strongest quadrupoles and sextupoles are positioned at the highest beta functions in the FFS, naturally the IR contains many high-order aberrations. We compute the third-order and fourth-order driving terms in the collider. The cancellation of the resonances at third-order remains intact. But the fourth-order resonance driving terms become much larger as shown in Fig. 8. Clearly, the aberrations in the IR are dominant in the entire ring.

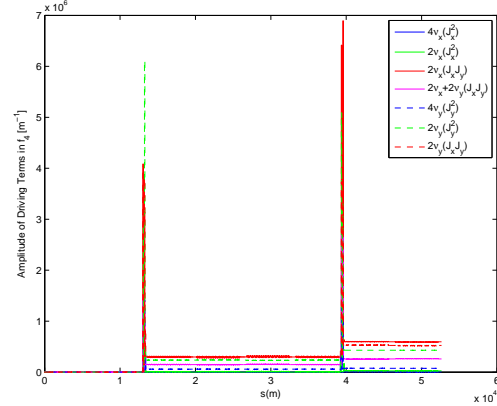


Figure 8: Fourth-order resonances driving terms in the collider with two interaction regions.

To quantify their nonlinear effects in the collider, we compute the tune shifts, the high-order chromaticities, and geometric and chromatic tune shifts using the normal form analysis and tabulate the results in Table 7. The table shows that the geometric-chromatic tune shifts are at the same level at $\delta = 0.01$ than the geometric tune shifts. This result is achieved by adding a few octupoles and decapoles at the beta peaks in the interaction regions.

Finally, we evaluate the dynamic aperture of the collider by tracking the particles with various momentums. The tracking is carried out with synchrotron oscillation and

Table 7: The nonlinear chromaticities and tune shifts due to betatron amplitudes in the collider that contains two interaction regions.

Derivatives of tunes	Values
$\partial v_{x,y}/\partial\delta$	0, 0
$\partial^2 v_{x,y}/\partial\delta^2$	-167, +790
$\partial^3 v_{x,y}/\partial\delta^3$	+27978, -19146
$\partial v_x/\partial J_x [m^{-1}]$	-8.18×10^4
$\partial v_{x,y}/\partial J_{y,x} [m^{-1}]$	-4.03×10^5
$\partial v_y/\partial J_y [m^{-1}]$	$+6.09 \times 10^4$
$\partial^2 v_x/\partial\delta\partial J_x [m^{-1}]$	-2.23×10^6
$\partial^2 v_{x,y}/\partial\delta\partial J_{y,x} [m^{-1}]$	-8.95×10^7
$\partial^2 v_y/\partial\delta\partial J_y [m^{-1}]$	-1.49×10^7

the radiation damping. The orbit and optics errors due to the saw-tooth energy profile are corrected by tapering the settings for all magnetic elements. As shown in Fig. 9, though the degradation of the off-momentum aperture is large, there is sufficient momentum acceptance to retain the particles in the long tail distribution of energy due to beamstrahlung. Most importantly, there is large enough dynamic aperture in the vertical plane to accommodate the large tail generated by the beam-beam interaction.

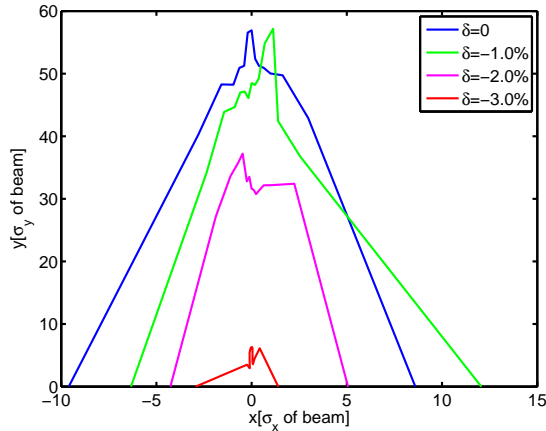


Figure 9: Dynamic aperture of the collider with various momentum deviations.

CONCLUSION

We have analyzed the impact on lattice design due to beamstrahlung in a Circular Higgs Factory. In particular, we found that a minimum emittance is necessary to retain an adequate beam lifetime. As a result, we developed a systematic procedure that can be applied to the lattice design.

Furthermore, we have developed a method to effectively compensate nonlinear chromaticity in the final focusing sys-

tem. In particular, we have demonstrated that the chromatic aberration can be reduced down to the required level in the arcs.

We have achieved 2% momentum acceptance in a lattice with an ultra-low beta interaction region. Six families of sextupoles are used in the chromatic correction. Octupoles and decapoles in the final focusing system are helpful to correct high order chromatic-geometric aberrations.

As shown in our paper, a Circular Higgs Factory requires not only a final focusing system with an ultra-low beta at the interaction point but also a very low-emittance lattice at very high energy. Such optics in a collider with a consistent set of accelerator parameters and especially with a large momentum aperture has been demonstrated in design.

ACKNOWLEDGMENT

I would like to thank Alex Chao, Yuri Nosochkov, Katsunobu Oide, Richard Talman, Uli Wienands, and Frank Zimmermann for many stimulating discussions. Special thanks to Professor Henry Tye for his hospitality during my visit in the Institute for Advanced Study in the Hong Kong University of Science and Technology.

REFERENCES

- [1] F. Amman and D. Ritson, "Design of electron-positron colliding beam rings," 1961 Internat. Conf. on High Energy Accelerators, Brookhaven, p471, (1961).
- [2] J.T. Seeman, "Beam-beam interaction: luminosity, tails and noise," SLAC-PUB-3182, July (1983).
- [3] "PEP-II: An Asymmetric B Factory", Conceptual Design Report, SLAC-418, June 1993.
- [4] "KEKB B-factory Design Report", KEK-Report-95-7, (1995).
- [5] B. Richter, "Very high electron-positron colliding beams for the study of weak interactions," Nucl. Instr. Meth. **136** p47 (1976).
- [6] V.I. Telnov, "Restriction on the energy and luminosity of e^+e^- storage rings due to beamstrahlung," Phys. Rev. Lett. **110**, 114801 (2013).
- [7] Yunhai Cai, "Single-particle dynamics in electron storage rings with extremely low emittance", Nucl. Instr. Meth. **A645**, p168 (2011).
- [8] K.L. Brown and R.V. Servranckx, "Optics modules for circular accelerator design," Nucl. Instr. Meth., **A258**, p480 (1987).
- [9] E. Forest, M. Berz, and J. Irwin, "Normal form methods for complicated periodic systems: a complete solution using differential algebra and Lie operators," Part. Accel. **24** 91 (1989).
- [10] Yunhai Cai, "Symplectic maps and chromatic optics in particle accelerators", Nucl. Instr. Meth. **A797**, p172 (2015).
- [11] M. Berz, "Differential Algebra Description of Beam Dynamics to Very High Order," Part. Accel. **24**, 109 (1989).